Aerodynamic Design of a Folded Krüger Device for a HLFC Wing

Dirk M. Franke and Jochen Wild

Abstract This work presents the design of a folded Krüger device under realistic geometrical requirements for a wing with hybrid laminar flow control (HLFC). A focus is laid on the investigation of the trade-off between space allocation of the retracted Krüger and the aerodynamic high-lift performance. The results reveal that the Krüger device is able to replace a reference slat device in relation to its aerodynamic high-lift performance. Further on the reduction of the allocation space influences the high-lift performance unfavorably.

1 Introduction

Over the last decades the cost for fuel for transport aircrafts has increased significantly, further on the need for environmental friendly aircrafts has come into political focus [1, 2]. These issues demand new techniques to decrease the high consumption and costs for energy. The laminar technology offers great potential to decrease the aerodynamic friction drag during cruise. However the laminar technology is sensitive to surface imperfections and contaminations (e.g. insects), which lead to an undesired transition from laminar to turbulent flow and consequently to unfavorable higher friction drag. These issues explain why the classical leading edge high-lift system namely slat, as regularly used, does not suit to this technology anymore and Krüger devices become an appealing alternative. Especially the shielding of the leading edge of the main element during take-off and landing against contamination and an upper surface without imperfections are realizable with a Krüger device.

D.M. Franke (✉) · J. Wild
German Aerospace Center, Institute of Aerodynamics and Flow Technology,
Lilienthalplatz 7, 38108 Braunschweig, Germany
e-mail: d.franke@dlr.de

J. Wild
e-mail: jochen.wild@dlr.de

A. Dillmann et al. (eds.), *New Results in Numerical and Experimental Fluid Mechanics X*, Notes on Numerical Fluid Mechanics and Multidisciplinary Design 132, DOI 10.1007/978-3-319-27279-5_2

In this work we consider hybrid laminar flow control (HLFC) which artificially generates laminar flow by a suction system in the area of the leading edge. A comprehensive report about the appliance, potential and drawbacks of HLFC was presented by NASA [3] in 1982.

In a further report of the NASA [4] from 1999 a flight demonstrator with a HLFC system is introduced. It was a full scale experiment, in which a 22 ft section of a Boeing 757 wing was redesigned, equipped with a HLFC system (suction panel, support structure, ducts and valves) and two slat elements were replaced by folded Krüger devices. The HLFC system was designed to permit flights to test the HLFC system at high Reynolds numbers.

This paper presents the design of a folded Krüger device as developed within the European Commision (EC) project DeSiReH [5, 6] for a transport aircraft. A key aspect of this work is the investigation of the trade-off between space allocation of the retracted Krüger device and the aerodynamic high-lift performance. Within this aerodynamic design task geometrical requirements are taken into account which are related to integration and space allocation issues for the HLFC system (e.g. suction panel) and the kinematics for the Krüger device. To investigate the trade-off between aerodynamic high-lift performance and space allocation multiple optimizations are conducted which differ in the spatial clearance of the retracted bull nose towards the upper shell of the wing. The goal of the aerodynamic Krüger design is to meet at least the high-lift performance of a reference slat device, that is designed by Airbus Germany, under fulfilling the geometrical requirements to realize a feasible HLFC system.

The aims of this publication are firstly to design a feasible Krüger device under realistic geometrical requirements with an enhanced high-lift performance and secondly to provide knowledge w.r.t. the trade-off (space allocation vs. high-lift performance). The evaluations of the aerodynamics are performed in two dimensions, in the front-spar normal system.

2 Methods

Figure 1 sketches the process chain for the optimization of the Krüger device that is embedded in the optimization environment CHAeOPS [7, 8]. The optimization environment runs on a Linux system. The preparation and extraction of the two dimensional airfoil is done in the computer aided design (CAD) environment CATIA V5R20 on a Windows system. The mesh generation process and the flow solver run sequentially on a Linux system.

Test Case: The underlying geometry is an outer wing section of a HLFC wing of a typical size of a wide-body transport aircraft. The wing is designed to allow laminar flow with a suction system. The investigated section is in the area of the outboard wing section with the most significant geometrical constraints and no trailing edge high-lift system is accounted for. The section has a spanwise length of 2.5 m within

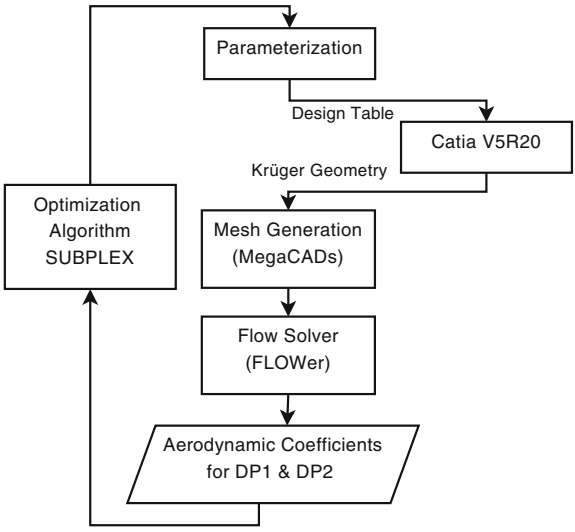

Fig. 1 Process chain of optimization

the optimization. The airfoil and Krüger shape are extracted in chord wise direction at the outboard position of the HLFC section. Afterwards the configuration is sweep scaled with the front-spar angle.
The free stream conditions for the design point in the front-spar-normal system read:

Design point 1 (DP1): $Ma_{2D} = 0.17$, $Re_{2D} = 12.0e+6$, p, T, ρ @ sea-level, $c_{l,max}$ evaluation.
Design Point 2 (DP2): $Ma_{2D} = 0.21$, $Re_{2D} = 14.8e+6$, $\alpha = 10°$, p, T, ρ @ sea-level.

The Reynolds-number is based on the front-spar normal chord length. In total three independent optimizations are performed, with differences in the spatial clearance of the retracted bull nose towards the upper shell of the wing.

Parameterization: The Krüger concept and geometrical description follows the concept of a folding bull-nose slotted Küger as developed within EC FP7 project DeSiReH. Within the optimization seven parameters are varied to control the shape and setting of the device. The parameters used for the definition of the shape and setting of the Krüger device are listed in Table 1, with a distinction if the parameter contributes to the setting or shape of the Krüger device. Additionally the table summarizes the parameters that are constant or indirectly defined within the optimization. Figure 2 illustrates the function of the most relevant parameters. The domains of the parameters are constant for all spatial clearances of the retracted bull nose towards the upper shell of the wing.

Geometrical Constraints: Geometrical constraints are implied to guarantee basic integration feasibility and functionality. Requirements are defined according to a segregation rule, thickness of the suction panel and to an assumption for the size of gooseneck bearing of the kinematics from the company that designs the kinematics,

Table 1 Parameters for the folded Krüger device

Parameter name	Setting parameter	Shape parameter	Remark
Shielding clearance, Δ_{SH}	x		
Overlap, ovl_K	x		
Hinge line offset, S_{HL}	x		
Front spar clearance, Δ_{FS}		x	
Bull nose height, l_B		x	
Bull nose fraction, $\mathrm{y}_{N,B}$		x	
Bull nose inflect, $\mathrm{x}_{N,B}$		x	
Shielding angle, δ_S	x		const.
Hinge line clearance, Δ_{HL}	x		const.
Thickness of suction panel, d_{skin}	x		const.
Trailing edge thickness, t_{TE}		x	const.
Bull spar height, d_k		x	const. in relation to panel length
Spatial clearance of retracted bull nose towards upper shell of the wing, Δ_B		x	const. for each optimization
Deflection angle, δ_K	x		indirectly defined
Bull nose width, h_B		x	indirectly defined

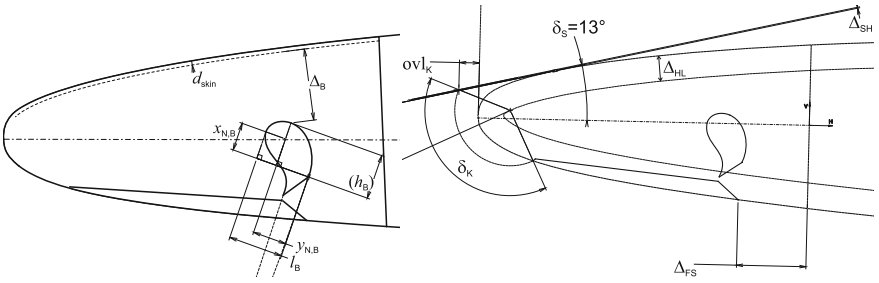

Fig. 2 *left* Sketch of the parameterization of the bull nose. *right* Sketch of the parameterization of the hinge line

namely ASCO Industries (www.asco.be). The thickness of the suction panel, the segregation rule and the size of the gooseneck define the hinge line clearance. Further on for the hinge line offset the same requirements hold, however here the segregation rule is slightly relaxed for the outboard section, which is considered during the optimization. The size of the Krüger panel is bounded by a minimum clearance towards the front spar. The trailing edge thickness of the Krüger is defined according to design requirements from INVENT (www.invent-gmbh.de), which develops the structure of the Krüger bull nose and the Krüger panel. The shielding impact angle is defined by a requirement document by Airbus. An additional requirement from

ASCO is to constrain the bull nose height to achieve a minimal cross section at the leading edge ribs. The bull nose in retracted position has a height of approximately 60 % of the local height of the airfoil.

All the afore mentioned constraints are inherent in the generation of the CATIA model of the Krüger device. Consequently the CATIA model of the Krüger device is always feasible w.r.t. the mentioned geometrical constraints.

Optimization Algorithm: The optimization is performed with the SUBPLEX [9] algorithm which is a deterministic, gradient free optimization algorithm developed by Rowan. According to Rowan "the subplex method's approach is to decompose the problem into low-dimensional subspaces that the Simplex method can search efficiently."

As shown by the author [10], the SUBPLEX algorithm is suitable for high-lift optimization. The algorithm is characterized by a good handling of noisy functions and by a well convergence behavior against strongly different sensitivities of the parameters.

Computational Mesh: A high mesh quality is important to resolve the complex flow phenomena around a high-lift configuration. In this study a focus of the meshing process is laid on the smoothness of the mesh, boundary layer and wake resolution for changing Krüger shape and setting. The meshes are fully structured (structured multi block) with around 190,000 grid nodes. The topology of the mesh, the number of grid nodes and the resolution of the walls are constant throughout the optimization. The meshes are always generated from scratch with the mesh generation software MegaCADs [11]. The meshes are suitable for both computational fluid dynamics (CFD) solver FLOWer [12] and DLR-TAU code [13].

Flow Solver: For the prediction of the integral coefficients during the optimization of the Krüger device the flow solver FLOWer is used. During the optimization the flow was solved on the second coarsening level, to obtain faster turn-around times. For the recomputations of the integral coefficients for the final, optimized shapes the flow solver DLR-TAU code is used. With the DLR-TAU code computations were conducted on the fine mesh. Both codes solve the compressible, three-dimensional, unsteady Reynolds averaged Navier-Stokes (RANS) equations. The spatial approximation is done by a finite-volume method. In this work the one-equation turbulence model from Spalart Allmaras (SAO) [14] with central discretization, artificial scalar dissipation in fully turbulent mode is used. One significant difference between both codes is that FLOWer is developed for structured meshes whereas the DLR-TAU code is designed for unstructured meshes.

Optimization problem: The objective of the aerodynamic optimization problem is the maximization of the aerodynamic performance at high-lift conditions. The objective function of the problem is the weighted sum of the maximum lift coefficient at DP1 and the lift coefficient at DP2. A penalty term is added to the objective function if the maximum lift coefficient of the current design is worse than the maximum lift coefficient of the initial, baseline design. The objective function in mathematical notation reads:

$$
\begin{aligned}
&f_{\text{objective}} = -C_{l,DP1} - C_{l,DP2} + \text{Penalty}_{DP1},\\
&C_{l,DP1} = C_{l,max},\\
&C_{l,DP2} = C_l(\alpha = 10deg),\\
&\text{Penalty}_{DP1} = 0, \qquad\qquad if\ C_{l,DP1} \geq C_{l,DP1,\text{initial}}\\
&\text{Penalty}_{DP1} = 100 \cdot (C_{l,DP1,\text{initial}} - C_{l,DP1}), \quad if\ C_{l,DP1} < C_{l,DP1,\text{initial}}
\end{aligned}
$$

As described above the investigated designs within the optimization are always feasible w.r.t. the design requirements and geometrical constraints, respectively.

The aim of the design process is to meet at least the **Aerodynamic High-Lift Performance** of the slat which is related to:

- maximum lift coefficient ($c_{l,max}$),
- angle of attack of the maximum lift coefficient ($\alpha_{c_{l,max}}$),
- lift coefficient at a margin of 3° towards the angle of attack of the maximum lift coefficient ($c_l(\alpha_{c_{l,max}} - 3\ deg)$).

3 Results

Shape and Setting of Krüger device: The resulting, optimized shape and setting of the Krüger device for various bull nose clearances are shown in Fig. 3 left. Configuration V1 is the optimized design for a bull nose height clearance Δ_B of 100 mm, V2 for 115 mm and V3 for 125 mm. It is obvious that the different spatial clearances of the retracted bull nose have a significant influence on the final shape and setting. The overall length of the Krüger design V1 is higher than for V2 and V3. The two configurations V2 and V3 are comparable in their overall length of the Krüger device, but differ in their ratio of bull nose size and panel length. Configuration V2 has a

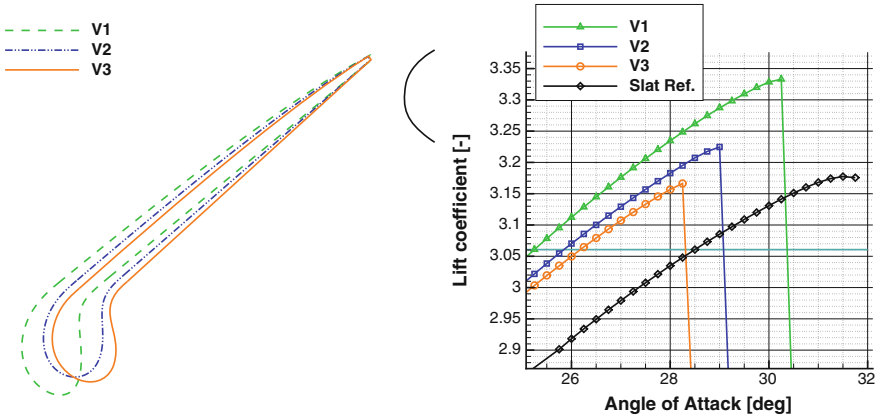

Fig. 3 *left* Shape and setting of optimized Krüger devices. *right* c_l-α curve for optimized Krüger and reference slat configurations at DP1

Table 2 Aerodynamic high-lift performance of optimized Krüger devices and reference slat device at DP1

Geometry	Bull nose clearance Δ_B (mm)	$c_{l,max,2D}$	$\alpha_{c_{l,max,2D}}$	$c_{l,2D}(\alpha_{c_{l,max,2D}} - 3\,deg)$
V1	100	3.33	30.25°	3.19
V2	115	3.22	29.0°	3.07
V3	125	3.17	28.25°	3.00
Slat	–	3.18	31.5°	3.06

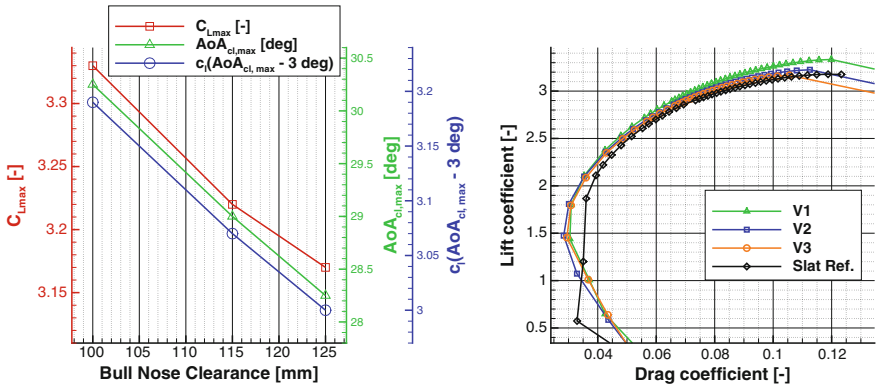

Fig. 4 *left* Aerodynamic high-lift performance versus bull nose height clearance at DP1. *right* c_l-c_d curve for optimized Krüger and reference slat configurations at DP1

larger bull nose and less panel length. It is recognizable that the deflection angle of the designs increase from V3 to V2 and to V1. The positions of the trailing edges of the multiple designs are similar.

Aerodynamics: Figure 3 right shows the lift curves of the optimized Krüger devices and of the reference slat. The aerodynamic high-lift performance is summarized in Table 2. The reference slat has a similar maximum lift coefficient as configuration V3 but at a significant higher angle of attack. The slope of the lift curve in the linear region is steeper for the Krüger devices as for the slat. Hence configuration V3 produces less lift at the 3° margin as the slat device. Configuration V2 is similar as the slat in its 3° margin, but due to the steeper slope the maximum lift coefficient is higher. Configuration V1 overshoots the maximum lift coefficient and the lift at the 3° margin compared to the slat. For all optimized configurations the angle of attack at which the maximum lift coefficient takes place cannot be reached in relation to the slat device. Figure 4 left summarizes the aerodynamic high-lift performance again but in relation to the bull nose clearance. The graph shows that all three components of the aerodynamic high-lift performance decrease when the bull nose clearance is increased.

Figure 4 right shows the lift versus drag curves. It is apparent that the Krüger devices produce less drag from $C_l \approx 1.2$ up to the maximum lift coefficient. However

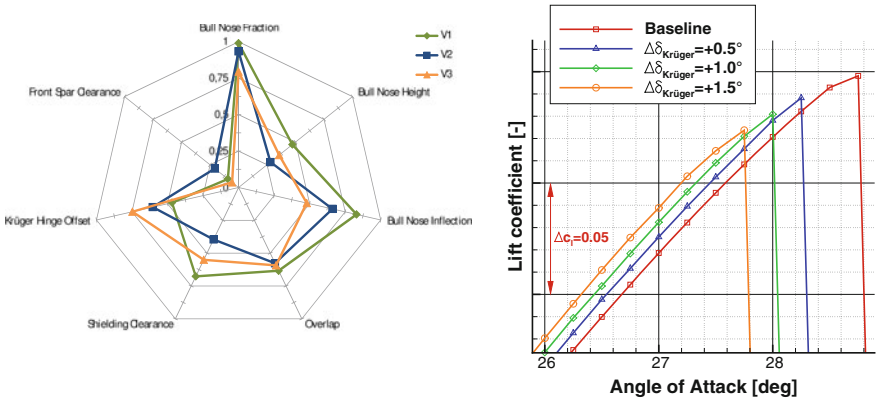

Fig. 5 *left* Distribution of the values of the parameters for configuration V1–V3 with normalized design spaces. *right* Lift coefficient over angle of attack for deflection angle variation on intermediate Krüger device at DP1

for smaller lift coefficients the drag coefficient increases strongly for the Krüger devices due to a fully separated pressure side of the airfoil in that angle of attack region.

The **Optimizations** are performed with at least three SUBPLEX cycles. A whole optimization with five SUBPLEX cycles took approximately 1 month on a single core of a workstation (Fujitsu Celsius R670-2, 2.4 GHz) with 340 optimization iterations. The distribution of the parameters for the optimized shape and setting of the Krüger devices are plotted in Fig. 5 left. According to this figure the parameters for the final designs are remote from the bounds of the parameter spaces, besides the parameters bull nose fraction for configuration V1, V2 and front spar clearance for configuration V1 and V3. During the optimizations only these two bounds of the parameter spaces were approached. All other bounds of the parameters stayed untouched.

4 Discussion

The results show that a trade-off between space allocation issues and aerodynamic high-lift performance is recognizable.

Shape and Setting of Krüger device and its influence on the **Aerodynamics**: Under consideration of the final designs V2 and V3 one can conclude that the panel length is of minor influence on the high-lift performance than the bull nose size. It seems that due to its larger bull nose, configuration V2 shows higher improvements for all three components of the high-lift performance. By increasing the panel length the optimizer tries to compensate the loss of the high-lift performance due to the limitation of the bull nose size but with minor achievements. An explanation for this observation is that for a bull nose with a bigger size the optimizer is able to shape the leading edge region with less maximum curvature so the flow can stay attached

up to higher angles of attack and consequently the maximum lift increases. Whereas the smaller bull nose is shaper (with higher curvature) in the leading edge region and hence the flow cannot follow the shape up to the same angle of attack. For all three designs the limitation of the lift augmentation is due to a separation of the suction side of the Krüger device.

The trailing edge position for all optimized configurations is very similar which is motivated in the constantly defined shielding angle and in the overlap which is rather similar for all three optimized settings. Additionally the shielding offset influences the trailing edge position, but due to its small domain the changes are marginally. Larger gaps/less overlap directly lead to shorter panels and flatter deflection.

A further aspect is the deflection angle, which is assumed to have a pronounced influence on the high-lift performance since the deflection angle increases also when the high-lift performance is increased (V3 to V2 to V1). Therefore a brief sensitivity study was performed to investigate the influence of the deflection angle, which is illustrated in Fig. 5 right. The sensitivity analysis was performed on an intermediate Krüger device. In this figure we see that the deflection angle is an important quantity. For the high-lift performance a reduction of the deflection angle is favorable w.r.t. the maximum lift coefficient, angle of attack of the maximum lift coefficient but unfavorable w.r.t. the margin of 3°. By this we can deduce that for the optimized shapes the reduction of the bull nose size which leads to a reduced high-lift performance is partly compensated by a reduction of the deflection angle.

Note, that the deflection angle is no free parameter, hence it is a dependent quantity which cannot be controlled directly during the optimization.

To conclude with the discussion of the shape, setting in relation to the aerodynamic performance the parameters with the most significant impact on the high-lift performance of the Krüger device are the deflection angle and the bull nose size. Additionally it can be stated that the slat device can be replaced by a Krüger device while maintaining the maximum lift coefficient and the lift coefficient at the 3° margin when enough allocation space is available. Only the angle of attack domain is reduced.

Optimization: By experience, distinct improvements are achieved in the first two SUBPLEX cycles, which means that the results are representative and reflect well the possible achievable improvements.

Parameterization: We can conclude that the domain of the parameters is sufficiently in its size, only for two parameters (front spar clearance, bull nose fraction) an extension of the parameter space may be favorable, if possible.

5 Conclusions and Outlook

The aim of the present publication to design a feasible Krüger device under realistic requirements is successfully accomplished. It is shown that a reference slat device can be replaced almost equally w.r.t. its aerodynamic high-lift performance. The

goal to investigate the trade-off between space allocation and aerodynamic high-lift performance is achieved. As shown, the bull nose size is a significant quantity for the aerodynamic high-lift performance. The reduction of the allocation space for the retracted bull nose has to be paid by a decrease in the aerodynamic high-lift performance.

Further tasks in this context are the verification of the two dimensional results for the three dimensional wing section. Additionally the design of the kinematics and the structure for the Krüger Bull nose and panel will be done by ASCO and INVENT.

Acknowledgments This work is supported by the European Community's Seventh Framework Program FP7 under grant agreement No 604013 through funding of the European project AFLoNext (www.aflonext.eu).

References

1. European Commission: European Aeronautics: A Vision for 2020. Luxembourg, Belgium, Office for Official Publications of the European Communities (2001)
2. European Commission: Fligthpath 2050 Europe's Vision for Aviation. Luxembourg, Belgium, Office for Official Publications of the European Communities (2011)
3. Boeing Commercial Airplane Company: Hybrid Laminar Flow Control Study. NASA/CR-165930 (1982)
4. Boeing Commercial Airplane Group: High Reynolds Number Hybrid Laminar Flow Control (HLFC) Flight Experiment III. Leading Edge Design, Fabrication, and Installation. NASA/CR-1999-209325 (1999)
5. Iannelli, P., Wild, J., Minervino, M., Moens, F., Raets, M.: Analysis and application of suitable CFD-based optimization strategies for high-lift system design. In: ECCOMAS 2012, Proceedings on CD-ROM, paper no. 2833 (2012)
6. Iannelli, P., Wild, J., Minervino, M., Strüber, H., Moens, F., Vervliet, A.: Design of a high-lift system for a laminar wing. In: EUCASS 2013, July 2013, Münich, Germany, Proceedings on CD-ROM (2013)
7. Wild, J.: Multi-objective constrained optimisation in aerodynamic design of high-lift systems. Int. J. Comput. Fluid Dyn. **22**(3), 153–168, Taylor & Francis, doi:10.1080/10618560701868420, ISSN 1061-8562 (2008)
8. Wild, J., Brezillon, J., Amoignon, O., Quest, J., Moens, F., Quagliarella, D.: Advanced design by numerical methods and wind tunnel verification within the European high-lift program. J. Aircr. **46**(1), 157–167, ISSN 0021–8669 (2009)
9. Rowan, T.: Functional stability analysis of numerical algorithms. Dissertation. Department of Computer Sciences, University of Texas at Austin, USA (1990)
10. Wild, J.: Numerische Optimierung von zweidiminsionalen Hochauftriebskonfigurationen durch Lösung der Navier-Stokes-Gleichungen. Research Report 2001–11. DLR, Institute of Aerodynamics and Flow Technology (2001)
11. Brodersen, O., Ronzheimer, A., Ziegler, R., Kunert, T., Wild, J., Hepperle, M.: Aerodynamic Applications using MegaCads. In: Cross, M. et al. (eds.) 6th International Conference on Numerical Grid Generation, London (1998)
12. Raddatz, J., Fassbender, J.K.: Block structured Navier-Stokes solver FLOWer. In: MEGAFLOW—Numerical Flow Simulation for Aircraft Design, Springer, pp. 27–44, ISBN 3-540-24383-6 (2005)

13. Gerhold, T.: Overview of the Hybrid RANS Code TAU. In: MEGAFLOW—Numerical Flow Simulation for Aircraft Design. Notes on Numerical Fluid Mechanics and Multidisciplinary Design, Vol. 89 (2005)
14. Spalart, P.R., Allmaras, S.R.: A one-equation turbulence model for aerodynamic flows. Paper 1992–439, AIAA (1992)

http://www.springer.com/978-3-319-27278-8

New Results in Numerical and Experimental Fluid Mechanics X
Contributions to the 19th STAB/DGLR Symposium Munich, Germany, 2014
Dillmann, A.; Heller, G.; Krämer, E.; Wagner, C.; Breitsamter, C. (Eds.)
2016, XVI, 897 p. 544 illus., 279 illus. in color., Hardcover
ISBN: 978-3-319-27278-8